J. Fluid Mech. (2009), *vol.* 627, *pp.* 341–360.
doi:10.1017/S0022112009005965 Printed in the United Kingdom

Induced-charge electrokinetic flows about polarizable nano-particles: the thick-Debye-layer limit

MOHAMMAD ABU HAMED AND EHUD YARIV†

Department of Mathematics, Technion - Israel Institute of Technology, Haifa 32000, Israel

(Received 1 October 2008 and in revised form 25 December 2008)

Using the standard weak-field approximation, we analyse the steady-state electrokinetic flow about an uncharged ideally polarizable spherical particle for the case of a Debye thickness which is large compared with the particle size. The dimensionless problem is governed by two parameters: β, the applied field magnitude (normalized with the thermal scale), and λ, the Debye thickness (normalized with particle size). The double limit $\beta \ll 1$ and $\lambda \gg 1$ is singular, and the resolution of the flow field requires the use of inner–outer asymptotic expansions in the spirit of Proudman & Pearson (J. Fluid Mech., vol. 2, 1957, p. 237). Two asymptotic limits are identified: the 'moderately thick' limit $\beta\lambda \ll 1$, in which the outer domain is characterized by the Debye thickness, and the 'super-thick' limit $\beta\lambda \gg 1$, in which the outer domain represents the emergence of electro-migration in the leading-order ionic-transport process. The singularity is stronger in the comparable two-dimensional flow about a circular cylinder, where a switchback mechanism in the moderately thick limit modifies the familiar $O(\beta^2)$ leading-order flow to $O(\beta^2 \ln \lambda)$.

1. Introduction

Electrokinetic flows about polarizable particles have been studied in the Soviet and post-Soviet colloidal literature since the pioneering work of Levich (1962). In contrast to 'classical' electrokinetic phenomena, wherein the fixed surface charge density is a physicochemical property of the particle–electrolyte system (Saville 1977; Anderson 1989), flows about ideally polarizable (perfectly conducting) surfaces are characterized by mobile surface charge which is induced by the externally applied electric field (Simonov & Dukhin 1973; Shilov & Simonova 1981; Gamayunov, Murtsovkin & Dukhin 1986; Murtsovkin 1996). This phenomenon was re-discovered by Bazant & Squires (2004) who coined the term 'induced-charge' flows to describe the entire host of effects associated with field-induced charge redistributions about polarizable surfaces, as in AC electro-osmosis (Ramos *et al.* 1998; Ajdari 2000; Brown, Smith & Rennie 2000; González *et al.* 2000; Green *et al.* 2000; Wang *et al.* 2006) and electrohydrodynamic particle–electrode interactions (Böhmer 1996; Trau, Saville & Aksay 1996, 1997; Solomentsev, Böhmer & Anderson 1997; Sides 2001, 2003; Ristenpart, Aksay & Saville 2004, 2007*a*, *b*). Similar mechanisms also occur near ion-selective membranes and granules (Rubinstein & Shtilman 1979; Dukhin 1991; Rubinstein & Zaltzman 2001; Ben & Chang 2002; Ben, Demekhin & Chang 2004; Zaltzman & Rubinstein 2007).

† Email address for correspondence: yarive@technion.ac.il

Current research directions in this field include microfluidic applications (Bazant & Squires 2004; Zhao & Bau 2007*a*; Harnett *et al.* 2008), particle–wall (Zhao & Bau 2007*b*, Yariv 2009) and particle–particle (Saintillan 2008) interactions, non-spherical particles (Yariv 2005; Squires & Bazant 2006; Saintillan, Darve & Shaqfeh 2006*a*; Yossifon, Frankel & Miloh 2007; Yariv 2008*b*) and suspension dynamics (Saintillan *et al.* 2006*a*; Saintillan, Shaqfeh & Darve 2006*b*; Rose *et al.* 2007). As explained by Squires & Bazant (2004), induced-charge flows occur over all polarizable surfaces, the case of a perfectly conducting surface representing the extreme limit of an ideally polarizable material (see Yossifon *et al.* 2007). Accordingly, the induced-charge phenomenon is also pertinent in a variety of electrokinetic flows about dielectric surfaces (Thamida & Chang 2002; Yossifon, Frankel & Miloh 2006), as well as biological molecules and cells (Dukhin 1986).

Aside from several exceptions (Zhao & Bau 2007*b*), the common practice in induced-charge-flow analysis is to employ the thin-Debye-layer model, whereby the electrokinetic processes within the Debye layer are lumped into two bulk-scale boundary conditions (Keh & Anderson 1985; Anderson 1989). With the recent advancement in device miniaturization it is not uncommon however to encounter microfluidic systems in which the pertinent linear dimension is comparable to the Debye thickness. In this general class of problems, the familiar concepts associated with the thin-Debye-layer limit (zeta potential, slip velocity and Debye-layer capacitance) lose their concrete meaning. Accordingly, understanding this class cannot be achieved by extending the thin-layer model; rather, one needs to confront the full set of electrokinetic equations (Saville 1977).

Induced-charge flows at arbitrary Debye thickness were theoretically investigated using a weak-field approximation (Murtsovkin 1996; Simonova, Shilov & Shramko 2001). A systematic asymptotic analysis of that problem which also provided closed-form expressions for the attendant flow field was carried out by Yariv & Miloh (2008). This work was soon followed by generalizations to non-spherical particles and non-uniformly applied fields Miloh (2008).

Of special interest is the extreme case of Debye thickness which is *large* compared with the particle linear dimension, pertinent in nano-fluidics (Stein, Kruithof & Dekker 2004; Eijkel & Berg 2005; Schoch, Han & Renaud 2008) and in distilled low-salt-concentration solutions, where the Debye thickness can approach the micron scale (see (2.1)). At first sight, it may appear that the thick-layer limit could be obtained by properly degenerating the results of Yariv & Miloh (2008). However, as will become evident in subsequent analysis, this limit is a singular one, and requires inner–outer asymptotic expansions in the spirit of Proudman & Pearson (1957). Resolving this limit constitutes the aim of the present paper.

We focus upon the simplest configuration that exhibits the essential features of induced-charge flow: a perfectly conducting spherical particle which is exposed to a uniform electric current in an unbounded electrolyte solution. In dimensionless notation, this problem is characterized by two dimensionless parameters: β, the applied field magnitude (normalized with the thermal scale), and λ, the Debye thickness (normalized with the particle size). Following Saville (1977), we focus upon the double limit $\beta \ll 1$ and $\lambda \gg 1$. Note that the weak-field limit $\beta \ll 1$ in Saville's analysis represents a small perturbation to an already existing Debye cloud; in the present problem, on the other hand, the Debye-cloud charge scales as β.

The double limit is manipulated using regular-perturbation methods, in which the particle dimension constitutes a natural length scale. The weak-field limit relaxes the strong coupling of the governing equations, and leading-order solutions for the ionic

concentration and the electric potential are readily calculated. The ensuing velocity field, however, fails to decay at large distances from the particle. This failure implies that the asymptotic solution is non-uniform, indicating that a second length scale affects the problem (Van Dyke 1964). A systematic asymptotic solution therefore requires the use of inner–outer expansions (Hinch 1991), in which the inner scale describes processes occurring at particle neighbourhood. The choice of the outer scale reflects two possible asymptotic limits: the 'moderately thick' limit $1 \ll \lambda \ll 1/\beta$, and the 'super-thick' limit $\lambda \gg 1/\beta$. Both limits are investigated, but a full asymptotic solution is found only for the first.

We also analyse a comparable two-dimensional configuration – an infinite cylinder in an unbounded electrolyte solution. Cylindrical geometries have already been analysed in the context of 'fixed-charge' electrokinetics about non-polarizable surfaces (Keh & Chen 1993; Keh, Horng & Kuo 2006). These geometries are of special importance in induced-charge electrokinetic processes in microfluidic systems, where fixed bodies (e.g. nanowires) are abundant (Bazant & Squires 2004). This is indeed explicit in previous analyses – both theoretical (Squires & Bazant 2004; Zhao & Bau 2007*b*) and experimental (Levitan *et al.* 2005) – of two-dimensional configurations. The singularity in the two-dimensional problem is stronger than that in the comparable three-dimensional case, and a switchback mechanism actually reshuffles the asymptotic expansions in the inner region.

The paper is organized as follows: In the next section we formulate the governing equations. The asymptotic analysis is outlined in § 3. The moderately thick limit is analysed in § 4, and the super-thick limit in § 5. The comparable two-dimensional problem of an infinite cylinder is discussed in § 6. Concluding remarks are given in § 7.

2. Problem formulation

An uncharged spherical particle (radius a) is suspended in a symmetric z–z electrolyte solution (viscosity μ, permittivity ϵ). The solution is neutral, whereby the cations and anions number density is equal, say n_∞. The particle is a perfect conductor, and is chemically inert: the solution ions cannot discharge on its surface.

At time zero, a uniform electric field E_∞ is externally applied at large distances from the particle. After a short transient (Squires & Bazant 2004; Yossifon, Frankel & Miloh to appear), the system reaches a steady state in which the solution becomes charged in the near-particle region (the Debye layer). Our interest lies in the steady-state electrokinetic processes – and especially the flow field – which is established throughout the fluid domain.

We employ a dimensionless formulation. Length variables are normalized by a; the ionic concentrations $n_\pm$ are obtained by normalizing with n_∞; the electric potential is naturally normalized with the thermal voltage $\varphi_T = kT/ze$ (kT being the Boltzmann factor and e the elementary charge) – about 25 mV for a univalent solution. The Poisson equation already possesses a natural length scale, namely the Debye thickness. Thus, the dimensionless Debye thickness λ, defined by

$$\lambda^2 = \frac{\epsilon kT}{2z^2e^2a^2n_\infty}, \tag{2.1}$$

readily emerges as a governing parameter. Another parameter,

$$\beta = \frac{aE_\infty}{\varphi_T}, \tag{2.2}$$

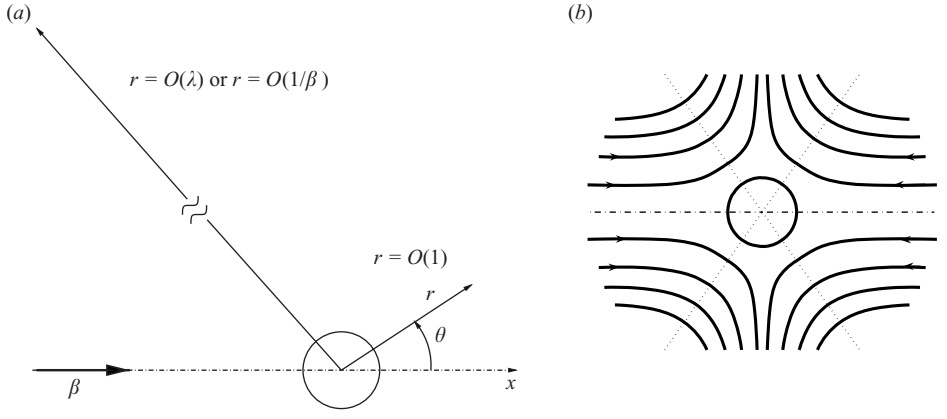

FIGURE 1. (*a*) The particle geometry and dimensionless coordinates. Also shown is a qualitative schematic illustration of the inner and outer asymptotic regions. (*b*) Streamlines ($\psi = \text{const.}$) at the meridian plane for $\lambda = 5$, drawn using (4.26). Also shown are the front ($\theta = \theta_0$) and back ($\theta = \pi - \theta_0$) cones that separate the inflow and outflow regions.

reflects the applied field magnitude. The balance between viscous friction and Coulomb body forces yields the velocity scale

$$\mathscr{U} = \frac{zean_\infty \varphi_T}{\mu}. \tag{2.3}$$

The pressure is accordingly normalized with $\mu\mathscr{U}/a$. In several references (Saville 1977; Yariv & Miloh 2008) the velocity is normalized by the electrokinetic speed $\epsilon\varphi_T^2/\mu a$. The present scale differs from it by a $2\lambda^2$ factor and is more suitable for the limit $\lambda \gg 1$.

The normalization procedure results in a dimensionless formulation for the ionic densities $n_\pm$, the electric potential φ, the velocity field $\boldsymbol{v}$ and the pressure p. In prescribing the boundary conditions, we employ a spherical coordinate system (r, θ, ϖ), $r = 0$ coinciding with the particle centre and $\theta = 0$ along the applied field (see figure 1*a*). We also define the symmetry axis x, whose positive direction coincides with $\theta = 0$. The equatorial plain is chosen as $x = 0$.

As is common in the literature we assume that both the cations and anions possess the same ionic diffusivity D. While the central asymptotic results in the present investigation are independent of this assumption, we retain it in favour of brevity. The ionic concentrations $n_\pm$ are therefore governed by the conservation equations

$$\nabla \cdot (\nabla n_\pm \pm n_\pm \nabla\varphi) = \frac{\alpha}{2\lambda^2}\, \boldsymbol{v} \cdot \nabla n_\pm \tag{2.4}$$

wherein the dimensionless group $\alpha = \epsilon\varphi_T^2/\mu D$ is independent of particle size; in view of particle impermeability to mass (see (2.14)), they also satisfy the no-flux conditions

$$\frac{\partial n_\pm}{\partial r} \pm n_\pm \frac{\partial \varphi}{\partial r} = 0 \qquad \text{at} \quad r = 1; \tag{2.5}$$

moreover, both concentrations must approach the equilibrium density at large distances from the particle

$$n_\pm \to 1, \qquad \text{as} \quad r \to \infty. \tag{2.6}$$

The electric potential φ is governed by Poisson's equation,

$$\nabla^2\varphi = -\frac{q}{2\lambda^2}, \tag{2.7}$$

wherein

$$q = n_+ - n_- \tag{2.8}$$

is the volumetric charge density (normalized with zen_∞); it must also acquire a uniform value on the conducting particle surface, whence with no loss of generality we also require

$$\varphi = 0 \quad \text{at} \quad r = 1; \tag{2.9}$$

at large distance, moreover, it must asymptotically approach the appropriate expression for the uniformly applied field

$$\varphi \sim -\beta r\cos\theta \qquad \text{as} \quad r \to \infty. \tag{2.10}$$

The velocity field is incompressible

$$\nabla\cdot\boldsymbol{v} = 0 \tag{2.11}$$

and it satisfies the Stokes equation, accounting for the Coulomb body force,

$$\nabla^2\boldsymbol{v} - \nabla p = q\nabla\varphi, \tag{2.12}$$

By forming its curl, the latter can be formulated in terms of the fluid vorticity, $\boldsymbol{\omega} = \nabla\times\boldsymbol{v}$

$$\nabla^2\boldsymbol{\omega} = \nabla q\times\nabla\varphi; \tag{2.13}$$

in view of the particle impermeability to mass and the no-slip condition, the velocity vanishes on the particle boundary

$$\boldsymbol{v} = \boldsymbol{0} \quad \text{at} \quad r = 1, \tag{2.14}$$

and it also decays at large distances from the particle

$$\boldsymbol{v} \to \boldsymbol{0} \qquad \text{as} \quad r \to \infty. \tag{2.15}$$

Lastly, one needs to impose a consistency condition (Yariv 2005, 2008*a*; Yariv & Miloh 2008). Since the particle was uncharged to begin with, and given its impermeability to ions, its total charge remains zero (though it may possess a non-uniform charge density). Using the boundary condition representation of Gauss law, this integral constraint appears as

$$\oint_{r=1} \mathrm{d}A\,\frac{\partial\varphi}{\partial r} = 0. \tag{2.16}$$

Equations (2.4)–(2.16) uniquely determine the steady-state transport process.

Instead of the ionic concentrations $n_\pm$, it is sometimes useful to employ the charge density q and the total ionic concentration

$$c = n_+ + n_-; \tag{2.17}$$

thus, addition of (2.4) yields the 'salt balance' equation,

$$\nabla\cdot(\nabla c + q\nabla\varphi) = \frac{\alpha}{2\lambda^2}\,\boldsymbol{v}\cdot\nabla c, \tag{2.18}$$

whereas subtraction of (2.4) yields the charge balance equation,

$$\nabla\cdot(\nabla q + c\nabla\varphi) = \frac{\alpha}{2\lambda^2}\,\boldsymbol{v}\cdot\nabla q. \tag{2.19}$$

Similarly, the boundary conditions (2.5) may be written equivalently as

$$\frac{\partial c}{\partial r} + q\frac{\partial \varphi}{\partial r} = 0, \quad \frac{\partial q}{\partial r} + c\frac{\partial \varphi}{\partial r} = 0 \quad \text{at} \quad r = 1, \tag{2.20}$$

and the far-field conditions (2.6) appear as

$$c \to 2, \quad q \to 0 \qquad \text{as} \quad r \to \infty. \tag{2.21}$$

The solenoidal and axisymmetric attributes of $\boldsymbol{v}$ allow it to be derived from a stream function ψ (Happel & Brenner 1965)

$$\boldsymbol{v} = \frac{1}{r\sin\theta}\hat{\boldsymbol{e}}_{\varpi} \times \nabla\psi; \tag{2.22}$$

substitution into (2.13) yields

$$\mathrm{E}^4\psi = \left(\frac{\partial q}{\partial r}\frac{\partial \varphi}{\partial \theta} - \frac{\partial q}{\partial \theta}\frac{\partial \varphi}{\partial r}\right)\sin\theta, \tag{2.23}$$

wherein

$$\mathrm{E}^2 = \frac{\partial^2}{\partial r^2} + \frac{\sin\theta}{r^2}\frac{\partial}{\partial \theta}\left(\frac{1}{\sin\theta}\frac{\partial}{\partial \theta}\right). \tag{2.24}$$

In addition to this equation, ψ also satisfies the impermeability and no-slip conditions on the particle boundary

$$\psi = \frac{\partial \psi}{\partial r} = 0 \qquad \text{at} \quad r = 1 \tag{2.25}$$

and the far-field condition

$$\psi/r^2 \to 0 \qquad \text{as} \quad r \to \infty, \tag{2.26}$$

reflecting the velocity attenuation at large distances.

The preceding equations are coupled and highly nonlinear. Yet, several symmetries associated with reflection about the equatorial plane $x = 0$ may be extracted without the need to actually solve them: it is evident from the structure of the differential equations and boundary conditions that φ, q and the axial velocity component are odd functions of x, while c, p and the transverse velocity component are even functions of x. It is convenient to represent this symmetry in spherical coordinates, where $\boldsymbol{v}$ adopts the form $\hat{\boldsymbol{e}}_r u + \hat{\boldsymbol{e}}_\theta v$. Here, u and v are the radial and circumferential velocity components, and $\{\hat{\boldsymbol{e}}_r, \hat{\boldsymbol{e}}_\theta, \hat{\boldsymbol{e}}_{\varpi}\}$ are the unit vectors in spherical coordinates. It is readily verified that c, u and p are invariant under the transformation $\theta \to \pi - \theta$, while φ, q and v change their sign. Specifically, that implies that

$$n_-(\theta) = n_+(\pi - \theta). \tag{2.27}$$

Note that these symmetry properties hold only for initially uncharged particles (see (2.16)).

For typical values appropriate to aqueous solutions ($\epsilon \approx 6 \times 10^{-10}$ kg m s^{-2} V^{-2}, $\mu \approx 10^{-6}$ kg m^{-1} s^{-1}) and characteristic values of ionic diffusivities (10^{-9} m^2 s^{-1}) α is about 0.5. We therefore proceed assuming α to be an $O(1)$ parameter. The other parameters appearing in the governing equations are λ and β. Even for strongly applied fields, β is usually small in view of typical dimensions of colloidal particles (Saville 1977; Yariv & Miloh 2008); this tendency is only intensified when considering nano-particles, and we accordingly assume $\beta \ll 1$. In this paper, we consider the double

limit

$$\lambda \gg 1, \quad \beta \ll 1. \tag{2.28}$$

3. Asymptotic analysis

Since the applied field is the driver of the electrokinetic transport, we postulate the following expansions

$$\varphi \sim \beta\varphi^{(0)} + \cdots, \tag{3.1}$$

$$q \sim \beta q^{(0)} + \cdots. \tag{3.2}$$

The momentum balance is animated by $O(\beta^2)$ body forces, whence we propose the expansion

$$\boldsymbol{v} \sim \beta^2 \boldsymbol{v}^{(1)} + \cdots, \tag{3.3}$$

together with comparable expansions for p, $\boldsymbol{\omega}$ and ψ. The forcing term in the salt balance (2.18) is also $O(\beta^2)$; in view of (2.21) we anticipate the expansion

$$c \sim 2 + \beta^2 c^{(1)} + \cdots. \tag{3.4}$$

Poisson's equation implies that $\varphi^{(0)}$ is harmonic

$$\nabla^2 \varphi^{(0)} = 0. \tag{3.5}$$

Applying the boundary condition (2.9) and the far-field condition (2.10) yields

$$\varphi^{(0)} = -\left(r - \frac{1}{r^2}\right)\cos\theta + \frac{A}{r} - A. \tag{3.6}$$

The integral constraint (2.16) then yields $A = 0$. The leading $O(\beta)$ balance of (2.19) implies that $q^{(0)}$ is also harmonic. The boundary conditions at $r = 1$ and $r \to \infty$ then yield the dipole solution

$$q^{(0)} = -3\frac{\cos\theta}{r^2}. \tag{3.7}$$

When focusing upon the electrokinetic flow, no need arises for calculating the salt distribution $c^{(1)}$. In view of (3.2) and (3.4), the inner expansions for the ionic concentrations are

$$n_\pm \sim 1 + \beta n_\pm^{(0)} + \cdots \tag{3.8}$$

in which

$$n_+^{(0)} = -n_-^{(0)} = \tfrac{1}{2} q^{(0)}. \tag{3.9}$$

Consider now the flow problem. The leading-order velocity field is solenoidal

$$\nabla \cdot \boldsymbol{v}^{(1)} = 0 \tag{3.10}$$

and satisfies the $O(\beta^2)$ momentum balance:

$$\nabla^2 \boldsymbol{v}^{(1)} - \nabla p^{(1)} = q^{(0)} \nabla \varphi^{(0)}. \tag{3.11}$$

In addition, it vanishes at $r = 1$ and attenuates at large distances away from the particle.

Even before attempting to solve these equations we readily observe a problem: the Coulomb body forces in (3.11) decay at an r^{-2} rate, therefore resulting in a velocity field which does not attenuate at infinity. This implies that the double limit (2.28)

is singular. This singularity is indeed apparent from the solution of the flow field. Substitution of (3.6) and (3.7) into (2.23) yields

$$\mathrm{E}^4\psi^{(1)} = \frac{18}{r^2}\mathscr{C}_3(\cos\theta), \tag{3.12}$$

where

$$\mathscr{C}_3(\eta) = \frac{\eta(1-\eta^2)}{2} \tag{3.13}$$

is the Gegenbauer function of order 3 and degree $-1/2$ (Happel & Brenner 1965). Seeking a solution of the form

$$\psi^{(1)}(r,\theta) = f^{(1)}(r)\mathscr{C}_3(\cos\theta) \tag{3.14}$$

we find that $f^{(1)}$ satisfies the ordinary differential equation

$$\mathscr{L}f^{(1)} = \frac{18}{r^2}, \tag{3.15}$$

where

$$\mathscr{L} = \frac{\mathrm{d}^4}{\mathrm{d}r^4} - \frac{12}{r^2}\frac{\mathrm{d}^2}{\mathrm{d}r^2} + \frac{24}{r^3}\frac{\mathrm{d}}{\mathrm{d}r}. \tag{3.16}$$

This equation possesses the particular integral

$$f_P^{(1)} = \frac{3r^2}{4} \tag{3.17a}$$

and the homogeneous solution

$$f_H^{(1)} = g_5 r^5 + g_3 r^3 + g_0 + \frac{g_{-2}}{r^2}. \tag{3.17b}$$

Note that the particular integral (3.17*a*) does not satisfy (2.26); moreover, this failure cannot be remedied by any of the terms of the homogeneous solution.

Clearly, the mathematical reason for the above impasse is the slow $1/r^2$-type decay of the charge density. This decay rate, and the consequent inability to satisfy the velocity-decay condition, reflects a non-uniformity of the asymptotic solution. This non-uniformity is triggered by the existence of another length scale in addition to the particle dimension a. The present analysis is only valid within an $r = O(1)$ inner region, and must be supplemented by a comparable analysis at an appropriate 'outer' region quantified by a large scale. In the present problem there are actually two such scales, λ and $1/\beta$. The outer scaling is determined by the smallest of these two. Two cases are therefore pertinent (see figure 1*a*): the 'moderately thick' limit $1 \ll \lambda \ll 1/\beta$, and the 'super-thick' limit $1 \ll 1/\beta \ll \lambda$.

In view of the scale disparity, the velocity field $\boldsymbol{v}^{(1)}$ is no longer required to decay at large r. Thus, we do not apply (2.26) to $\psi^{(1)}$; rather, the four integration constants appearing in (3.17) are to be determined from the boundary condition (2.25) and from matching with the outer velocity field, yet to be determined.

4. The moderately thick limit

We begin with the moderately thick limit, $1 \ll \lambda \ll 1/\beta$. At $O(\lambda)$ distances the Debye layer affects the electric potential: the approximation (3.5), giving rise to the slow charge attenuation rate, breaks down and a transition occurs to an exponential charge attenuation.

To analyse the Debye-scale processes, we define the outer radial variable R, appropriate for $r = O(\lambda)$, by normalization with the Debye thickness

$$r = \lambda R. \tag{4.1}$$

The outer region is therefore described by $R = O(1)$.

The outer fields are denoted by capital symbols. With $\nabla_R = \lambda\nabla$ being the outer gradient operator, Poisson's equation appears as

$$\nabla_R^2 \Phi = -\frac{Q}{2}; \tag{4.2}$$

the salt and charge balances are

$$\nabla_R \cdot (\nabla_R C + Q\nabla_R \Phi) = \frac{\alpha}{2\lambda} \boldsymbol{V} \cdot \nabla_R C, \tag{4.3}$$

$$\nabla_R \cdot (\nabla_R Q + C\nabla_R \Phi) = \frac{\alpha}{2\lambda} \boldsymbol{V} \cdot \nabla_R Q, \tag{4.4}$$

and the flow equations adopt the form

$$\nabla_R \cdot \boldsymbol{V} = 0, \quad \nabla_R^2 \boldsymbol{V} - \lambda\nabla_R P = \lambda Q \nabla_R \Phi. \tag{4.5}$$

The fields are subjected to the far-field limits

$$C \to 2, \quad Q \to 0, \quad \boldsymbol{V} \to \boldsymbol{0} \qquad \text{as} \quad R \to \infty. \tag{4.6}$$

and to the requirement of a uniform field at infinity

$$\Phi \sim -\beta\lambda R\cos\theta \qquad \text{as} \quad R \to \infty. \tag{4.7}$$

Additionally, the outer variables must match the comparable inner fields.

The governing equations suggest the following asymptotic expansions:

$$\Phi \sim -\beta\lambda R\cos\theta + \delta(\beta, \lambda)\Phi^{(0)} + \cdots, \quad Q \sim \delta(\beta, \lambda)Q^{(0)} + \cdots, \tag{4.8}$$

where the pre-factor $\delta(\ll \beta\lambda)$ remains to be determined. The momentum balance then suggests that $\boldsymbol{V}$ is $O(\beta\lambda^2\delta)$ and the salt balance suggests the expansion

$$C \sim 2 + \beta\lambda\delta(\beta, \lambda)C^{(0)} + \cdots. \tag{4.9}$$

In the limit $\delta \ll \beta\lambda \ll 1$ we then find that the leading-order charge density is not affected by electro-migration with the leading-order electric field, nor by fluid convection:

$$\nabla_R^2 Q^{(0)} + 2\nabla_R^2 \Phi^{(0)} = 0. \tag{4.10}$$

Substitution into the above of the $O(\delta)$ Poisson equation

$$\nabla_R^2 \Phi^{(0)} = -\frac{Q^{(0)}}{2} \tag{4.11}$$

yields the following Helmholtz equation:

$$\nabla_R^2 Q^{(0)} = Q^{(0)}. \tag{4.12}$$

The general solution that decays at large R is given by the eigenfunction expansion

$$Q^{(0)} = R^{-1/2} \sum_{n=0}^{\infty} A_n K_{n+1/2}(R) P_n(\cos\theta). \tag{4.13}$$

The need to match (3.7) implies, however, that A_1 is the only coefficient that does not vanish. Using the small-argument expansion for the modified Bessel functions

(Abramowitz & Stegun 1965)

$$K_{n+1/2}(z) \sim \frac{1}{2}\Gamma\left(n+\frac{1}{2}\right)\left(\frac{z}{2}\right)^{-n-1/2} \quad \text{as} \quad z \to 0, \tag{4.14}$$

and matching with the inner charge field (3.7) yields $A_1 = -3(2/\pi)^{1/2}$ and

$$\delta = \frac{\beta}{\lambda^2}. \tag{4.15}$$

The latter is indeed smaller then $\beta\lambda$, thus confirming the consistency of our asymptotic scheme. The velocity is therefore $O(\beta^2)$

$$\boldsymbol{V} \sim \beta^2 \boldsymbol{V}^{(1)} + \cdots. \tag{4.16}$$

As in the inner region, we define a stream function (cf. (2.22))

$$\boldsymbol{V} = \frac{1}{R\sin\theta}\hat{\boldsymbol{e}}_{\varpi} \times \nabla_R \Psi. \tag{4.17}$$

Clearly, Ψ possesses the asymptotic expansion

$$\Psi \sim \beta^2 \Psi^{(1)} + \cdots. \tag{4.18}$$

Substitution of the leading-order electric field and charge density into the outer momentum balance, followed by a derivation similar to the one performed in the inner region, yields (cf. (3.12)) the differential equation (wherein the operator E_R^2 is given by (2.24) with r replaced by R)

$$\mathrm{E}_R^4 \Psi^{(1)} = 6\mathrm{e}^{-R}\left(1+\frac{3}{R}+\frac{3}{R^2}\right)\mathscr{C}_3(\cos\theta) \tag{4.19}$$

and the far-field condition

$$R \to \infty: \quad \Psi^{(1)}/R^2 \to 0. \tag{4.20}$$

We seek a solution of the form

$$\Psi^{(1)} = F^{(1)}(R)\mathscr{C}_3(\cos\theta). \tag{4.21}$$

The function $F^{(1)}(R)$ is governed by the ordinary differential equation

$$\mathscr{L}_R F^{(1)} = 6\mathrm{e}^{-R}\left(1+\frac{3}{R}+\frac{3}{R^2}\right), \tag{4.22}$$

in which $\mathscr{L}_R$ is given by (3.16) with r replaced by R. The homogeneous solution of this equation has a functional form similar to (3.17*b*); the far-field decay condition (4.20) implies that both the R^5 and R^3 powers must be rejected. Using the variation-of-parameters method, we then obtain

$$F^{(1)}(R) = 6\mathrm{e}^{-R}\left(1+\frac{3}{R}+\frac{3}{R^2}\right) + \frac{G_{-2}}{R^2} + G_0, \tag{4.23}$$

where G_{-2} and G_0 are constants of integration which are to be determined via matching with the inner solution (3.17).

In view of the stretching (4.1), the requirement of velocity matching implies that the large-r expansion of ψ must match the small-R expansion of $\lambda^2\Psi$. Expanding (4.23) for small R yields (this requires five terms in the Taylor approximation of e^{-R})

$$F^{(1)} \sim \frac{18+G_{-2}}{R^2} + G_0 - 3 + \frac{3}{4}R^2 + O(R^3). \tag{4.24}$$

Inspection of (3.17) shows that the comparable inner field $f^{(0)}$ is at least $O(r^2)$ at large r, and could even behave as r^3 or r^5 depending upon the coefficients g_3 and g_5 in the homogeneous solution (3.17*b*). Thus, matching is possible only if $G_{-2} = -18$ and $G_0 = 3$; since $F^{(0)}$ behaves like R^2 at small R, g_3 and g_5 must vanish. It is then readily verified that asymptotic matching indeed fulfilled to leading order. The remaining coefficients in (3.17*b*) are found using boundary condition (2.25), which readily yields $g_{-2} = 3/4$ and $g_0 = -3/2$.

The flow field in the entire fluid domain is conveniently represented by a uniformly valid approximation $\bar{\psi}$. Adding (3.14) and (4.21) and subtracting the overlapping parts yield the leading-order approximation

$$\bar{\psi}(r, \theta; \lambda) = \beta^2 \bar{f}(r; \lambda) \mathscr{C}_3(\cos\theta) + \cdots, \tag{4.25}$$

in which

$$\bar{f}(r; \lambda) = -\frac{3}{2} + \frac{3}{4r^2} + \lambda^2 \left[6\mathrm{e}^{-r/\lambda} \left(1 + \frac{3\lambda}{r} + \frac{3\lambda^2}{r^2} \right) - \frac{18\lambda^2}{r^2} + 3 \right]. \tag{4.26}$$

The corresponding streamlines in the meridian plain are shown in figure 1(*b*).

It is illuminating to compare the leading-order flow in the moderately thick limit with that corresponding to moderate λ values at weak fields (Yariv & Miloh 2008). While the moderately thick limit introduces a singular two-scale radial dependence, the latitudinal dependence upon θ is similar. Indeed, both the inner and outer flow profiles (3.14) and (4.21) represent a quadrupolar pump wherein fluid is pumped from the particle 'front' ($0 < \theta < \theta_0$) and 'back' ($\theta_0 < \theta < \pi$) cones, with $\cos\theta_0 = 1/3$, and ejected alongside the equatorial plain $\theta_0 < \theta < \pi - \theta_0$. This pump can be quantified by the net volumetric flux $\mathscr{F}$ (normalized with $a^2\mathscr{U}$) which enters into the back cone at large distances from the particle. Naively, one would be tempted to follow Yariv & Miloh (2008) and obtain $\mathscr{F}$ using the far-field behaviour of ψ

$$\mathscr{F} = -2\pi \lim_{r\to\infty} \psi(r, \pi - \theta_0). \tag{4.27}$$

This limit, however, does not exist. Indeed, the non-uniformity of the inner solution necessitates use of the uniform approximation (4.26) to capture the flux at large distances, whereby (4.27) is replaced by

$$\mathscr{F} = -2\pi \lim_{r\to\infty} \bar{\psi}(r, \pi - \theta_0). \tag{4.28}$$

Substitution of (4.26) yields

$$\mathscr{F} \sim \frac{2\pi\beta^2\lambda^2}{\sqrt{3}}. \tag{4.29}$$

This expression agrees with the large-λ limit of the general flux expression obtained by Yariv & Miloh (2008). (Recall the different velocity scale in that paper.)

5. The super-thick limit

We now consider the limit $1 \ll 1/\beta \ll \lambda$. Here, the non-uniformity of the inner solution stems from a different mechanism. Recall that the $1/r^2$ decay of $n_{\pm}^{(0)}$ reflects the dominance of the $O(\beta)$ diffusive term in (2.4) over the $O(\beta^2)$ electro-migration term. Consideration of the decay rate in these terms reveals, however, that this dominance break down at sufficiently large distances. Indeed, the $O(\beta/r^4)$ diffusive term decays faster than the $O(\beta^2/r^3)$ electro-migration term; regardless of how small

β is, at distances $O(1/\beta)$ these terms become comparable. This type of non-uniformity is mostly associated with inertia effects in low-Reynolds-number flows (Proudman & Pearson 1957), and is also familiar from low-Péclet-number problems of forced convection (Acrivos & Taylor 1962) and thermocapillarity (Subramanian 1981).

Thus, the appropriate scale for the super-thick limit is $1/\beta$. To analyse the processes occurring at $r = O(1/\beta)$ we define the radial variable ρ as (cf. (4.1))

$$r = \beta^{-1}\rho. \tag{5.1}$$

As in the moderately thick layer analysis, The outer fields are denoted by capital symbols. With $\nabla_\rho = \beta^{-1}\nabla$ being the outer gradient operator, Poisson's equation appears as (cf. (4.2))

$$\nabla_\rho^2 \Phi = -\frac{1}{2\beta^2\lambda^2} Q. \tag{5.2}$$

In the present limit, it is preferable to employ the ionic conservation equations, rather than those governing salt and charge. Transformation of (2.4) to outer variables yields

$$\nabla_\rho \cdot (\nabla_\rho N_\pm \pm N_\pm \nabla_\rho \Phi) = \frac{\alpha}{2\beta\lambda^2} \boldsymbol{V} \cdot \nabla_\rho N_\pm; \tag{5.3}$$

finally, the flow equations adopt the form (cf. (4.5))

$$\nabla_\rho \cdot \boldsymbol{V} = 0, \quad \beta\nabla_\rho^2 \boldsymbol{V} - \nabla_\rho P = Q\nabla_\rho \Phi. \tag{5.4}$$

The pertinent variables are subject to the far-field limits (4.6) and to the requirement of a uniform field at infinity (cf. (4.7))

$$\Phi \sim -\rho\cos\theta \qquad \text{as} \quad \rho \to \infty. \tag{5.5}$$

Additionally, they must match the comparable inner variables.

The governing equations suggest the following asymptotic expansions (cf. (4.8)):

$$\Phi \sim -\rho\cos\theta + \chi(\beta,\lambda)\Phi^{(0)} + \cdots, \quad N_\pm \sim 1 + \chi(\beta,\lambda)N_\pm^{(0)} + \cdots, \tag{5.6}$$

where the pre-factor $\chi(\ll 1)$ remains to be determined. We therefore anticipate that (cf. (4.8) and (4.9))

$$Q \sim \chi(\beta,\lambda)Q^{(0)} + \cdots, \quad C \sim 2 + \chi(\beta,\lambda)C^{(0)} + \cdots. \tag{5.7}$$

The momentum balance then suggests that $\boldsymbol{V}$ is $O(\chi/\beta)$. It is then readily verified that the ratio of convection to diffusion–migration is of order $\chi/\beta^2\lambda^2$. Since $\chi \ll 1$ so must be this factor. Accordingly, convection does not affect the leading-order ionic balances

$$\nabla_\rho^2 N_\pm^{(0)} = \pm\hat{\boldsymbol{e}}_x \cdot \nabla_\rho N_\pm^{(0)}. \tag{5.8}$$

The cation concentration $N_+^{(0)}$ satisfies a standard diffusion–convection equation. This equation was solved by Acrivos & Taylor (1962) in the context of forced convection

$$N_+^{(0)} = \exp\left(\frac{\rho\cos\theta}{2}\right)\rho^{-1/2}\sum_{n=0}^{\infty} S_n K_{n+1/2}\left(\frac{\rho}{2}\right) P_n(\cos\theta); \tag{5.9}$$

matching with the inner solution (see (3.8) and (3.9)) shows that S_1 is the only non-vanishing coefficient. Using the small-argument expansion (4.14) yields

$$S_1 = -\frac{3}{4\pi^{1/2}} \tag{5.10}$$

and

$$\chi = \beta^3. \tag{5.11}$$

Note that $\chi \ll 1$, *a posteriori* confirming the asymptotic procedure. Using (2.27), we finally find

$$Q^{(0)} = -\frac{3}{2\pi^{1/2}} \cosh\left(\frac{\rho\cos\theta}{2}\right) \rho^{-1/2} K_{3/2}\left(\frac{\rho}{2}\right) \cos\theta. \tag{5.12}$$

When considering the outer flow problem, we employ the expansions

$$\boldsymbol{V} \sim \beta^2 \boldsymbol{V}^{(1)} + \cdots, \quad P \sim \beta^3 P^{(1)} + \cdots. \tag{5.13}$$

The leading-order momentum balance is

$$\nabla_\rho^2 \boldsymbol{V}^{(1)} - \nabla_\rho P^{(1)} = -\hat{\boldsymbol{e}}_x Q^{(0)}. \tag{5.14}$$

Defining a stream function in the form (cf. (4.17))

$$\boldsymbol{V} = \frac{1}{\rho\sin\theta} \hat{\boldsymbol{e}}_\varpi \times \nabla_\rho \Psi, \tag{5.15}$$

and using the expansion

$$\Psi \sim \beta^2 \Psi^{(1)} + \cdots \tag{5.16}$$

yields the partial differential equation (cf. (4.19))

$$\mathrm{E}_\rho^4 \Psi^{(1)} = \frac{3}{4} \mathrm{e}^{-\rho/2} \left(1 + \frac{6}{\rho} + \frac{12}{\rho^2}\right) \cosh\left(\frac{\rho\cos\theta}{2}\right) \mathscr{C}_3(\cos\theta) \tag{5.17}$$

wherein the operator E_ρ^2 is given by (2.24) with r replaced by ρ. Unfortunately, we were unable to solve that equation. Without such a solution it is impossible to perform the requisite matching.

Regardless of the explicit form of the velocity field, it is clear that the charge distribution (5.12) (implicit in the forcing term of (5.17)) prohibits a quadrupolar pump structure, of the form existing in the moderately thick limit.

6. The flow about a perfectly conducting cylinder

We now consider another idealized geometry – an infinite cylinder of a circular cross-section (radius a). The applied field is directed perpendicular to the cylinder axis, and all the electrokinetic transport processes are two-dimensional. The problem is naturally handled via polar coordinates (r, θ), r and θ being the radial and azimuthal coordinates, with $\theta = 0$ in the direction of the applied field. These two coordinates possess a different geometric meaning than the coordinates r and θ appearing in the three-dimensional problem; nevertheless, the governing equations (2.4)–(2.21), developed originally for a spherical particle, remain valid.

To analyse the two-dimensional flow we employ the Helmholtz stream function (cf. (2.22)),

$$\boldsymbol{v} = \hat{\boldsymbol{e}}_z \times \nabla\psi, \tag{6.1}$$

where $\hat{\boldsymbol{e}}_z = \hat{\boldsymbol{e}}_r \times \hat{\boldsymbol{e}}_\theta$ is a unit vector in the direction of the cylinder axis. Substitution of the relation

$$\nabla^2 \boldsymbol{\omega} = \hat{\boldsymbol{e}}_z \nabla^4 \psi \tag{6.2}$$

into (2.13) yields the inhomogeneous bi-harmonic equation (cf. (3.12))

$$\nabla^4\psi = \frac{\partial q}{\partial r}\frac{\partial \varphi}{r\partial\theta} - \frac{\partial q}{r\partial\theta}\frac{\partial \varphi}{\partial r}. \tag{6.3}$$

The boundary condition (2.25) remain valid, but the velocity-decay condition (2.26) is modified to the form

$$\psi/r \to 0 \qquad \text{as} \quad r \to \infty. \tag{6.4}$$

It seems plausible to proceed with the asymptotic expansion (3.1)–(3.4). Following the same procedure as that applied to the sphere problem, we find (cf. (3.6) and (3.7))

$$\varphi^{(0)} = -\left(r - \frac{1}{r}\right)\cos\theta \tag{6.5a}$$

and

$$q^{(0)} = -\frac{4\cos\theta}{r}. \tag{6.5b}$$

As in the three-dimensional problem, the leading-order flow is governed by (3.10) and (3.11). With the Coulomb body forces in (3.11) decaying as $1/r$, the singularity is stronger compared with that appearing in the three-dimensional problem: the velocity field $\boldsymbol{v}^{(1)}$ actually diverges at large distances from the cylinder. The enhancement of non-uniformities in two-dimensional configurations is familiar to other Stokes-flow problems.

This singularity in the double limit (2.28) becomes explicit when attempting to evaluate $\psi^{(1)}$. Substitution of (6.5) into (6.3) yields

$$\nabla^4\psi^{(1)} = \frac{4}{r^2}\sin 2\theta. \tag{6.6}$$

Clearly, $\psi^{(1)}$ is of the form

$$\psi^{(1)}(r,\theta) = \tilde{f}^{(1)}(r)\sin 2\theta. \tag{6.7}$$

The function $\tilde{f}^{(1)}$ satisfies the ordinary differential equation (cf. (3.15))

$$\tilde{\mathscr{L}}\,\tilde{f}^{(0)} = \frac{4}{r^2}, \tag{6.8}$$

where (cf. (3.16))

$$\tilde{\mathscr{L}} = \frac{\mathrm{d}^4}{\mathrm{d}r^4} + \frac{2}{r}\frac{\mathrm{d}^3}{\mathrm{d}r^3} - \frac{9}{r^2}\frac{\mathrm{d}^2}{\mathrm{d}r^2} + \frac{9}{r^3}\frac{\mathrm{d}}{\mathrm{d}r}. \tag{6.9}$$

This equation possesses the homogeneous solution

$$\tilde{f}_H^{(1)} = \tilde{g}_4 r^4 + \tilde{g}_2 r^2 + \tilde{g}_0 + \frac{\tilde{g}_{-2}}{r^2}, \tag{6.10a}$$

and the particular integral

$$\tilde{f}_P^{(1)} = -\frac{r^2}{4}\ln r. \tag{6.10b}$$

Note that the particular integral (6.10*b*) does not satisfy (6.4). Again, we encounter a non-uniform solution.

As in the three-dimensional problem, the preceding solution represents the electrokinetics in an inner region $r = O(1)$. We here only consider the moderately thick limit $\beta\lambda \ll 1$. The outer region is again defined by $R = O(1)$, with R (now a polar coordinate) again defined by the stretching (4.1). The governing equations

(4.2)–(4.7) remain valid, as are the expansions (4.8) and (4.9) and the leading-order equations (4.10)–(4.12). The two-dimensional solution of (4.12) that decays at large R is

$$Q^{(0)} = \sum_{n=0}^{\infty} K_n(R)(\tilde{A}_n \cos n\theta + \tilde{B}_n \sin n\theta). \tag{6.11}$$

The need to match the inner charge (6.5*b*) implies that $\tilde{A}_1$ is the only coefficient that does not vanish. Using the small-argument expansion of the modified Bessel function (Abramowitz & Stegun 1965) and matching with (6.5*b*) yields $\tilde{A}_1 = -4$ and (cf. (4.15))

$$\delta = \frac{\beta}{\lambda}. \tag{6.12}$$

The latter is indeed smaller then $\beta\lambda$, thus confirming the consistency of our asymptotic scheme. The outer velocity field is therefore $O(\beta^2\lambda)$ (cf. (4.16))

$$\boldsymbol{V} \sim \beta^2\lambda \boldsymbol{V}^{(1)} + \cdots. \tag{6.13}$$

As in the inner region, we define a stream function

$$\boldsymbol{V} = \hat{\boldsymbol{e}}_z \times \nabla_R \Psi \tag{6.14}$$

wherein

$$\Psi \sim \beta^2\lambda \Psi^{(1)} + \cdots. \tag{6.15}$$

The leading-order momentum balance in the outer region is

$$\nabla_R^4 \Psi^{(1)} = 2K_2(R) \sin 2\theta. \tag{6.16}$$

Seeking a solution of the form $\Psi^{(1)} = F^{(1)}(R) \sin 2\theta$ we find that $F^{(1)}(R)$ is governed by the ordinary differential equation $\mathscr{L}_R F^{(1)} = 2K_2(R)$, in which $\mathscr{L}_R$ is provided by (6.9) with r replaced by R. The homogeneous solution of this equation has the functional form (6.10*a*); the far-field decay condition $\Psi^{(1)}/R \to 0$ implies however that both the R^4 and R^2 powers must be rejected. Using the variation-of-parameters method we then obtain

$$F^{(1)}(R) = \tilde{G}_0 + \frac{\tilde{G}_{-2}}{R^2} + 2K_2(R). \tag{6.17}$$

Here, G_0 and G_{-2} are constants of integration which are to be determined via matching with the inner solution.

Definitions (6.1) and (6.14) in conjunction with (4.1) imply that the large-r expansion of ψ must match the small-R expansion of $\lambda\Psi$. Using the small-argument expansion of the modified Bessel functions (Abramowitz & Stegun 1965) we find for $R \ll 1$:

$$F^{(1)}(R) \sim \frac{\tilde{G}_{-2} + 4}{R^2} + (\tilde{G}_0 - 1) - \frac{R^2}{4} \ln R + \frac{\ln 2 - \gamma + 3/4}{4} R^2 + O(R^4 \ln R), \tag{6.18}$$

in which γ is Euler's constant. In view of (3.17*a*), the comparable inner field $f^{(1)}$ is at least $O(r^2 \ln r)$ at large r, and could even behave as r^4 if the coefficient $\tilde{g}_4$ in the homogeneous solution (6.10*a*) does not vanish. Thus, matching is possible only if $\tilde{G}_{-2} = -4$ and $\tilde{G}_0 = 1$; since $F^{(1)}$ then behaves like $R^2 \ln R$ at small R, $\tilde{g}_4$ must consequently vanish.

Rewriting (6.18) in terms of the inner variable r yields

$$\lambda^2 F^{(1)}(R) \sim \frac{\ln \lambda}{4} r^2 + \frac{\ln 2 - \gamma + 3/4}{4} r^2 - \frac{r^2 \ln r}{4} + \cdots. \tag{6.19}$$

The last term in (6.19) neatly matches the problematic particular integral (3.17*a*); the comparable leading-order term, however, does not match (6.10). It therefore becomes evident that the inner asymptotic expansion (3.3) must be revised to

$$\boldsymbol{v} \sim \beta^2 \ln \lambda \, \boldsymbol{v}^{(0)} + \beta^2 \boldsymbol{v}^{(1)} + \cdots \tag{6.20}$$

with a comparable expansion for ψ. (It is easily verified that preceding analysis, and, specifically, the negligence of ionic convection in the calculation of $q^{(1)}$, remains valid.) Clearly, $\psi^{(0)}$ possesses the form $\tilde{f}^{(0)}(r)\sin 2\theta$, in which $\tilde{f}^{(0)}(r)$ is a homogeneous solution of $\mathscr{L}$ (cf. (6.10*a*))

$$\tilde{f}^{(0)} = \tilde{h}_4 r^4 + \tilde{h}_2 r^2 + \tilde{h}_0 + \frac{\tilde{h}_{-2}}{r^2}. \tag{6.21}$$

Matching with (6.19) is only possible if $\tilde{h}_4$ vanishes. We then readily obtain

$$\tilde{g}_2 = \frac{\ln 2 - \gamma + 3/4}{4}, \quad \tilde{h}_2 = \frac{1}{4}. \tag{6.22}$$

Since we considered two asymptotic orders that differ by a logarithmic factor, we have effectively followed the 1–1 van Dyke matching rule (Van Dyke 1964). The appearance of a leading asymptotic order in the inner region, which is triggered by matching rather than by scaling arguments, is known as 'switchback' (Hinch 1991).

The remaining coefficients in (6.10*a*) and (6.21) are found using the boundary condition (2.25). Applying it to $\psi^{(1)}$ yields $\tilde{g}_0 = 1/2$ and $\tilde{g}_{-2} = -1/4$, while applying it to $\psi^{(0)}$ yields

$$\tilde{h}_0 = \frac{\ln 2 - \gamma + 1/2}{2}, \quad \tilde{h}_{-2} = -\frac{\ln 2 - \gamma + 1/4}{4}, \tag{6.23}$$

thereby completing the velocity calculation.

7. Concluding remarks

When considering electrokinetic flows about polarizable particles of realistic dimensions, both the thin and thick Debye-layer limits are somewhat idealized. Nevertheless, their understanding is useful in obtaining a qualitative picture of the transport processes occurring at intermediate values of the Debye thickness. The thin-layer limit is reasonably understood; in this paper we present a first analysis of the thick-layer limit. In an attempt to understand the electrokinetic processes in that limit, we have naturally focused upon the simplest induced-charge configuration: the steady-state electrokinetic flow about an ideally polarizable (perfectly conducting) spherical particle of zero net charge, which is exposed to a constant and uniform electric field.

We analysed the flow in the double limit of weak field and thick Debye layer. The evaluation of the Debye-layer structure appears to require a regular-perturbation scheme, in the spirit of Yariv & Miloh (2008). However, the failure to calculate the attendant velocity field indicates that the problem is inherently singular. We therefore resort to inner–outer asymptotic expansions, wherein the outer length scale depends upon the magnitude of the dimensionless group $\beta\lambda$. Two asymptotic limits are identified: the moderately thick limit $\beta\lambda \ll 1$, wherein the outer region is on the λ-scale, and the super-thick limit $\beta\lambda \gg 1$, where it is on the scale $1/\beta$. A full calculation of the inner flow field, at the particle scale, requires a preliminary analysis of the appropriate outer region followed by asymptotic matching. This goal is achieved in the

moderately thick limit, thereby yielding a complete calculation of the electrokinetic fields in both regions. The comparable analysis of the super-thick limit is frustrated by the inability to obtain an analytic solution for the outer momentum balance (5.17). We have also analysed the moderately thick limit for the two-dimensional geometry of an infinite cylinder. Here the non-uniformity of the inner solution is stronger; consequently, asymptotic matching results in a switchback effect which modifies the leading-order scaling of the inner flow. The different far-field behaviour in the two sub-limits is of obvious importance to subsequent analyses of wall effects (Gangwal *et al.* 2008; Saintillan in preparation; Yariv to appear).

The present analysis can be extended in several directions. Some of them, like the generalization to dielectric particles or AC fields, are rather technical. A challenging extension which is of clear practical interest involves relaxing the assumption of a weakly applied field, and perhaps even considering the extreme limit of strongly applied field. Initial electrokinetic analysis in the strong-field régime, wherein the flow field is assumed absent, has already appeared in the literature (Chu & Bazant 2006).

Another extension involves the analysis of charged particles. The present assumption of zero initial particle charge, in conjunction with the integral charge conservation argument (2.16), implies that the (uniform) particle electric potential is that of its undisturbed background. When the particle carries net charge, integral conservation arguments may introduce nonlinear potential shift (Dukhin, Vincent & Mozes 1993; Yariv 2008*a*). The vanishing of the particle potential in the present context guarantees several symmetries of the pertinent physical fields. The symmetry of the electric and velocity fields actually ensures that the particle does not experience any electrical or hydrodynamic force. This symmetry was implicitly employed in the analysis, where it was tacitly assumed that the particle remained stationary (see (2.14)).

The situation is of course quite different in the simplest configuration of charged *non-polarizable* particle, where the determination of the particle electrophoretic velocity is the natural goal. The electrophoretic velocity of a non-polarizable spherical particle in the thick-layer limit was originally calculated by Hückel (1924). It is obtained from a simple balance between the Coulomb force on a charged particle and a Stokes drag (Saville 1977). The determination of this velocity to $O(\beta)$ does not require any detailed calculations of the velocity fields. It is only when higher-order correction to this velocity are sought that singular perturbation theory becomes necessary. Such an investigation appears to constitute a formidable task: thus far, systematic singular-perturbation analyses of fixed-charge electrokinetics in the thick-Debye-layer limit have been performed only for an equilibrium Debye cloud (Natarajan & Schechter 1986), in the absence of an applied field.

REFERENCES

Abramowitz, M. & Stegun, I. A. 1965 *Handbook of Mathematical Functions*, 3rd edn. Dover.

Acrivos, A. & Taylor, T. D. 1962 Heat and mass transfer from single spheres in stokes flow. *Phys. Fluids* **5** (4), 387–394.

Ajdari, A. 2000 Pumping liquids using asymmetric electrode arrays. *Phys. Rev.* E **61** (1), R45–R48.

Anderson, J. L. 1989 Colloid transport by interfacial forces. *Annu. Rev. Fluid Mech.* **30**, 139–165.

Bazant, M. Z. & Squires, T. M. 2004 Induced-charge electrokinetic phenomena: theory and microfluidic applications. *Phys. Rev. Lett.* **92** (6).

Ben, Y. & Chang, H. C. 2002 Nonlinear Smoluchowski slip velocity and micro-vortex generation. *J. Fluid Mech.* **461**, 229–238.

Ben, Y., Demekhin, E. A. & Chang, H. C. 2004 Nonlinear electrokinetics and "superfast" electrophoresis. *J. Colloid Interface Sci.* **276**, 483–497.

Böhmer, M. 1996 In situ observation of 2-dimensional clustering during electrophoretic deposition. *Langmuir* **12**, 5747–5750.

Brown, A. B. D., Smith, C. G. & Rennie, A. R. 2000 Pumping of water with ac electric fields applied to asymmetric pairs of microelectrodes. *Phys. Rev.* E **63** (1), 016305.

Chu, K. T. & Bazant, M. Z. 2006 Nonlinear electrochemical relaxation around conductors. *Phys. Rev.* E **74**, 11501.

Dukhin, A. S. 1986 Pair interaction of disperse particles in electric-field. 3. Hydrodynamic interaction of ideally polarizable metal particles and dead biological cells. *Colloid J. USSR* **48**, 376–381.

Dukhin, S. S. 1991 Electrokinetic phenomena of the 2nd kind and their applications. *Adv. Colloid Interface* **35**, 173–196.

Dukhin, A. S., Vincent, B. & Mozes, N. 1993 Biospecific mechanism of double layer formation and peculiarities of cell electrophoresis. *Colloid Surface* A **73**, 29–48.

Eijkel, J. & Berg, A. 2005 Nanofluidics: what is it and what can we expect from it? *Microfluid. Nanofluid.* **1**, 249–267.

Gamayunov, N. I., Murtsovkin, V. A. & Dukhin, A. S. 1986 Pair interaction of particles in electric-field. 1. Features of hydrodynamic interaction of polarized particles. *Colloid J. USSR* **48** (2), 197–203.

Gangwal, S., Cayre, O., Bazant, M. & Velev, O. 2008 Induced-charge electrophoresis of metallodielectric particles. *Phys. Rev. Lett.* **100**, 58302.

González, A., Ramos, A., Green, N. G., Castellanos, A. & Morgan, H. 2000 Fluid flow induced by nonuniform ac electric fields in electrolytes on microelectrodes. II. A linear double-layer analysis. *Phys. Rev.* E **61** (4), 4019–4028.

Green, N. G., Ramos, A., González, A., Morgan, H. & Castellanos, A. 2000 Fluid flow induced by nonuniform ac electric fields in electrolytes on microelectrodes. I. Experimental measurements. *Phys. Rev.* E **61** (4), 4011–4018.

Happel, J. & Brenner, H. 1965 *Low Reynolds Number Hydrodynamics*. Prentice-Hall.

Harnett, C., Templeton, J., Dunphy-Guzman, K., Senousy, Y. & Kanouff, M. 2008 Model based design of a microfluidic mixer driven by induced charge electroosmosis. *Lab Chip* **8** (4), 565–572.

Hinch, E. J. 1991 *Perturbation Methods*. Cambridge University Press.

Hückel, E. 1924 The cataphoresis of the sphere. *Phys. Z.* **25**, 204–210.

Keh, H. J. & Anderson, J. L. 1985 Boundary effects on electrophoretic motion of colloidal spheres. *J. Fluid Mech.* **153**, 417–439.

Keh, H. & Chen, S. 1993 Diffusiophoresis and electrophoresis of colloidal cylinders. *Langmuir* **9** (4), 1142–1149.

Keh, H., Horng, K. & Kuo, J. 2006 Boundary effects on electrophoresis of colloidal cylinders. *J. Fluid Mech.* **231**, 211–228.

Levich, V. G. 1962 *Physicochemical Hydrodynamics*. Prentice-Hall.

Levitan, J., Devasenathipathy, S., Studer, V., Ben, Y., Thorsen, T., Squires, T. & Bazant, M. 2005 Experimental observation of induced-charge electro-osmosis around a metal wire in a microchannel. *Colloids Surface* A **267** (1–3), 122–132.

Miloh, T. 2008 Dipolophoresis of nanoparticles. *Phys. Fluids* **20**, 107105.

Murtsovkin, V. A. 1996 Nonlinear flows near polarized disperse particles. *Colloid J.* **58** (3), 341–349.

Natarajan, R. & Schechter, R. S. 1986 The solution of the nonlinear Poisson-Boltzmann equation for thick, spherical double-layers. *J. Colloid Interface Sci.* **113** (1), 241–247.

Proudman, I. & Pearson, J. R. A. 1957 Expansions at small Reynolds number for the flow past a sphere and a circular cylinder. *J. Fluid Mech.* **2**, 237–531.

Ramos, A., Morgan, H., Green, N. & Castellanos, A. 1998 AC electrokinetics: a review of forces in microelectrode structures. *J. Phys. D: Appl. Phys.* **31**, 2338–2353.

Ristenpart, W. D., Aksay, I. A. & Saville, D. A. 2004 Assembly of colloidal aggregates by electrohydrodynamic flow: Kinetic experiments and scaling analysis. *Phys. Rev.* E **69**, 21405.

Ristenpart, W. D., Aksay, I. A. & Saville, D. A. 2007*a* Electrically driven flow near a colloidal particle close to an electrode with a Faradaic current. *Langmuir* **23**, 4071–4080.

Ristenpart, W. D., Aksay, I. A. & Saville, D. A. 2007*b* Electrohydrodynamic flow around a colloidal particle near an electrode with an oscillating potential. *J. Fluid Mech.* **575**, 83–109.

Rose, K., Meier, J., Dougherty, G. & Santiago, J. 2007 Rotational electrophoresis of striped metallic microrods. *Phys. Rev.* E **75**, 11503.

Rubinstein, I. & Shtilman, L. 1979 Voltage against current curves of cation exchange membranes. *J. Chem. Soc. Farad. T. 2* **75**, 231–246.

Rubinstein, I. & Zaltzman, B. 2001 Electro-osmotic slip of the second kind and instability in concentration polarization at electrodialysis membranes. *Math. Mod. Meth. Appl. S.* **11**, 263–300.

Saintillan, D. 2008 Nonlinear interactions in electrophoresis of ideally polarizable particles. *Phys. Fluids* **20**, 067104.

Saintillan, D. In preparation. Nonlinear effects in electrophoresis of polarizable particles near rigid boundaries.

Saintillan, D., Darve, E. & Shaqfeh, E. S. G. 2006*a* Hydrodynamic interactions in the induced-charge electrophoresis of colloidal rod dispersions. *J. Fluid Mech.* **563**, 223–259.

Saintillan, D., Shaqfeh, E. S. G. & Darve, E. 2006*b* Stabilization of a suspension of sedimenting rods by induced-charge electrophoresis. *Phys. Fluids* **18** (12), 121503.

Saville, D. A. 1977 Electrokinetic effects with small particles. *Annu. Rev. Fluid Mech.* **9**, 321–337.

Schoch, R., Han, J. & Renaud, P. 2008 Transport phenomena in nanofluidics. *Rev. Mod. Phys.* **80**, 839–883.

Shilov, V. N. & Simonova, T. S. 1981 Polarization of electric double-layer of disperse particles and dipolophoresis in a steady (dc) field. *Colloid J. USSR* **43** (1), 90–96.

Sides, P. J. 2001 Electrohydrodynamic particle aggregation on an electrode driven by an alternating electric field normal to it. *Langmuir* **17**, 5791–5800.

Sides, P. J. 2003 Calculation of electrohydrodynamic flow around a single particle on an electrode. *Langmuir* **19**, 2745–2751.

Simonov, I. N. & Dukhin, S. S. 1973 Theory of electrophoresis of solid conducting particles in case of ideal polarization of a thin diffuse double-layer. *Colloid J. USSR* **35** (1), 191–193.

Simonova, T. S., Shilov, V. N. & Shramko, O. A. 2001 Low-frequency dielectrophoresis and the polarization interaction of uncharged spherical particles with an induced Debye atmosphere of arbitrary thickness. *Colloid J.* **63** (1), 108–115.

Solomentsev, Y., Böhmer, M. & Anderson, J. L. 1997 Particle clustering and pattern pormation during electrophoretic deposition: a hydrodynamic model. *Langmuir* **13**, 6058–6068.

Squires, T. M. & Bazant, M. Z. 2004 Induced-charge electro-osmosis. *J. Fluid Mech.* **509**, 217–252.

Squires, T. M. & Bazant, M. Z. 2006 Breaking symmetries in induced-charge electro-osmosis and electrophoresis. *J. Fluid Mech.* **560**, 65–101.

Stein, D., Kruithof, M. & Dekker, C. 2004 Surface-charge-governed ion transport in nanofluidic channels. *Phys. Rev. Lett.* **93**, 35901.

Subramanian, R. S. 1981 Slow migration of a gas bubble in a thermal gradient. *AIChE J.* **27**, 646–654.

Thamida, S. & Chang, H. C. 2002 Nonlinear electrokinetic ejection and entrainment due to polarization at nearly insulated wedges. *Phys. Fluids* **14**, 4315.

Trau, M., Saville, D. A. & Aksay, I. A. 1996 Field-induced layering of colloidal crystals. *Science* **272**, 706.

Trau, M., Saville, D. A. & Aksay, I. A. 1997 Assembly of colloidal crystals at electrode interfaces. *Langmuir* **13**, 6375–6381.

Van Dyke, M. 1964 *Perturbation Methods in Fluid Mechanics*. Academic press.

Wang, S., Chen, H., Lee, C., Yu, C. & Chang, H. 2006 AC electro-osmotic mixing induced by non-contact external electrodes. *Biosensors and Bioelectronics* **22** (4), 563–567.

Yariv, E. 2005 Induced-charge electrophoresis of nonspherical particles. *Phys. Fluids* **17** (5), 051702.

Yariv, E. 2008*a* Nonlinear electrophoresis of ideally polarizable spherical particles. *Europhys. Lett.* **82**, 54004.

Yariv, E. 2008*b* Slender-body approximations for electro-phoresis and electro-rotation of polarizable particles. *J. Fluid Mech.* **613**, 85–94.

Yariv, E. 2009 Boundary-induced electrophoresis of uncharged conducting particles: remote-wall approximations. *Proc. R. Soc.* A. **465**, 709–723.

Yariv, E. & Miloh, T. 2008 Electro-convection about conducing particles. *J. Fluid Mech.* **595**, 163–172.

Yossifon, G., Frankel, I. & Miloh, T. 2006 On electro-osmotic flows through microchannel junctions. *Phys. Fluids* **18**, 117108.

Yossifon, G., Frankel, I. & Miloh, T. 2007 Symmetry breaking in induced-charge electro-osmosis over polarizable spheroids. *Phys. Fluids* **19**, 068105.

Yossifon, G., Frankel, I. & Miloh, T. 2009 Macro-scale description of transient electro-kinetic phenomena over polarizable dielectric solids. *J. Fluid Mech.* **620**, 241–262.

Zaltzman, B. & Rubinstein, I. 2007 Electro-osmotic slip and electroconvective instability. *J. Fluid Mech.* **579**, 173–226.

Zhao, H. & Bau, H. 2007*a* Microfluidic chaotic stirrer utilizing induced-charge electro-osmosis. *Phys. Rev.* E **75**.

Zhao, H. & Bau, H. 2007*b* On the effect of induced electro-osmosis on a cylindrical particle next to a surface. *Langmuir* **23**, 4053–4063.